Structural Eng. / Earthquake Eng. Vol. 5. No. 1, 119s-127s. April 1988
Japan Society of Civil Engineers (Proc. of JSCE No. 392/I-9)

AN ANALYSIS OF ELASTO-PLASTIC BENDING OF RECTANGULAR PLATE

By Hiroshi MATSUDA and Takeshi SAKIYAMA***

In this paper, a discrete method for analyzing the problem of elasto-plastic bending of a rectangular plate is proposed. The solutions for partial differential equation of rectangular plate are obtained in discrete forms by applying numerical integration.

An incremental variable elasticity procedure has been used for the elasto-plastic analysis of the rectangular plate. As the applications of the proposed method, elasto-plastic bending of rectangular plate with four types of boundary conditions are calculated.

Keywords : rectangular plate, elasto-plastic bending, a discrete method

1. INTRODUCTION

The elasto-plastic bending problems of the rectangular plates have been analyzed by many researchers.

The upper- and lower-bounds ultimate capacities of the plate structures of perfectly plastic material can be determined with the theorems of limit analysis[1),2)].

The elasto-plastic behavior beyond the first yielding of the rectangular plate is analyzed by the direct numerical methods such as the finite difference methods[3)~5)], the discrete element methods[6)], the finite element methods[7)~9)], etc.[10),11)].

In this paper, a discrete method for analyzing the elasto-plastic bending problems of the rectangular plate is proposed. The discrete solutions of partial differential equations governing the elasto-plastic bending behavior of the rectangular plate are obtained in discrete forms, by transforming the differential equations into integral equations and applying numerical integrations, and they give the transverse shear forces, twisting moments, bending moments, rotations and deflections at all discrete points which are intersection of the vertical and horizontal equally dividing lines on the plate.

For the elasto-plastic analysis of the rectangular plate, an incremental variable elasticity procedure has been used. It is assumed that the Prandtl-Reuss' law, and the von Mises yield criterion are valid in this paper. In order to consider the extent of the yielded portions in the directions of the cross sections, the cross section of the plate is divided into many layers. As the application of the proposed method, numerical solutions for square plates with four types of boundary conditions : four simply supported edges, four clamped edges, two opposite edges simply supported and the other two edges clamped, and two opposite edges simply supported and the other two edges free, are presented. All four problems involve square

* Member of JSCE, Dr. Eng., Research Associate, University of Nagasaki (Nagasaki City, Nagasaki)
** Member of JSCE, Dr. Eng., Professor, University of Nagasaki (Nagasaki City, Nagasaki)

plates subjected to lateral loads that are uniformly distributed throughout the plate.

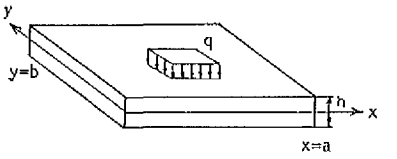

Fig. 1 Rectangular Plate and Coordinate System.

2. FUNDAMENTAL DIFFERENTIAL EQUATIONS

We consider a rectangular plate which is referred to as an x-y-z system of rectangular coordinates, and determine the position of the origin 0 of the x-y-z system at the corner of the middle plane of the plate as shown in Fig. 1. The surface of the plate are at $z=\pm h/2$, where h is the thickness of the plate. The transverse deflection and the rotations of the middle plane are denoted by w and θ_x, θ_y. If D is the flexural rigidity of the plate and E the modulus of elasticity, G the shear modulus of elasticity, ν the Poisson's ratio, κ the shear coefficient, Q_y and Q_x the transverse shear forces, M_{xy} the twisting moment, M_y and M_x the bending moments, then the fundamental differential equations governing the elasto-plastic bending of the rectangular plates which are subjected to the distributed lateral load $q(x, y)$ as shown in Fig. 1 are given as Eqs. (1. a)-(1. h). Since an incremental procedure is used, the fundamental differential equations are presented in incremental forms,

$$\frac{\partial \Delta Q_x}{\partial x}+\frac{\partial \Delta Q_y}{\partial y}+\Delta q=0 \cdots\cdots (1.\text{a}) \qquad \frac{\partial \Delta \theta_y}{\partial y}=\frac{1}{D}(b_{21}\Delta M_x+b_{22}\Delta M_y+b_{23}\Delta M_{xy}) \cdots\cdots (1.\text{e})$$

$$\frac{\partial \Delta M_x}{\partial x}+\frac{\partial \Delta M_{xy}}{\partial y}-\Delta Q_x=0 \cdots\cdots (1.\text{b}) \qquad \frac{\partial \Delta \theta_x}{\partial y}+\frac{\partial \Delta \theta_y}{\partial x}=\frac{1}{D}(b_{31}\Delta M_x+b_{32}\Delta M_y+b_{33}\Delta M_{xy}) \cdots\cdots (1.\text{f})$$

$$\frac{\partial \Delta M_y}{\partial y}+\frac{\partial \Delta M_{xy}}{\partial x}-\Delta Q_y=0 \cdots\cdots (1.\text{c}) \qquad \frac{\partial \Delta w}{\partial x}+\Delta \theta_x=\frac{\Delta Q_x}{\kappa G h} \cdots\cdots (1.\text{g})$$

$$\frac{\partial \Delta \theta_x}{\partial x}=\frac{1}{D}(b_{11}\Delta M_x+b_{12}\Delta M_y+b_{13}\Delta M_{xy}) \cdots\cdots (1.\text{d}) \qquad \frac{\partial \Delta w}{\partial y}+\Delta \theta_y=\frac{\Delta Q_y}{\kappa G h} \cdots\cdots (1.\text{h})$$

where $D=Eh^3/[12(1-\nu^2)]$, $G=E/[2(1+\nu)]$, $\kappa=5/6$, b_{ij} : APPENDIX I, ΔQ_y, ΔQ_x=increments of shear forces Q_y, Q_x; ΔM_{xy}, ΔM_y, ΔM_x=increments of moments M_{xy}, M_y, M_x; $\Delta \theta_y$, $\Delta \theta_x$=increments of rotations θ_y, θ_x; Δw=increment of deflection w, Δq=increment of load q.

By using the following non-dimensional expressions,

$X_1=a^2Q_y/[D_0(1-\nu^2)]$, $X_2=a^2Q_x/[D_0(1-\nu^2)]$, $X_3=aM_{xy}/[D_0(1-\nu^2)]$, $X_4=aM_y/[D_0(1-\nu^2)]$,
$X_5=aM_x/[D_0(1-\nu^2)]$, $X_6=\theta_y$, $X_7=\theta_x$, $X_8=w/a$, $\eta=x/a$, $\zeta=y/b$

the differential Eqs. (1. a)-(1. h) are rewritten as follows :

$$\sum_{s=1}^{8}\left[F_{1ts}\frac{\partial \Delta X_s}{\partial \zeta}+F_{2ts}\frac{\partial \Delta X_s}{\partial \eta}+F_{3ts}\Delta X_s\right]+\delta_{1t}\Delta \overline{q}=0 \cdots\cdots (2)$$

where δ is Kronecker's delta, a and b are length and width of the plate, $\overline{q}=\mu q_0 a^3/[D_0(1-\nu^2)][q(x, y)/q_0]$, q_0 is standard load intensity, $\mu=b/a$, $t=1, 2, \cdots, 8$ and F_{kts} is defined in Appendix II.

3. DISCRETE SOLUTIONS OF DIFFERENTIAL EQUATIONS

We divide a rectangular plate vertically into m equal-length parts and horizontally into n equal-length parts as shown in Fig. 2, and consider the plate as a group of discrete points which are the intersections of the vertical and horizontal dividing line.

The rectangular area, $0\leqq\eta\leqq\eta_i$ and $0\leqq\zeta\leqq\zeta_j$, corresponding to an arbitrary intersection (i, j) shown in Fig. 2, is expressed as the area $[i, j]$ in this paper, and the intersection (i, j) denoted by ⊙ is called the main point of the area $[i, j]$, and the intersections denoted by ○ as the inner dependent points, the intersections denoted by ● as the boundary dependent

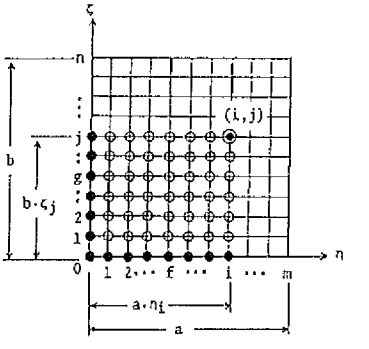

Fig. 2 Discrete Points on Rectangular Plate.

points.

By integrating Eq. (2) over the area $[i, j]$, the following integral equation is obtained.

$$\sum_{s=1}^{8}\left\{F_{1ts}\int_0^{\eta_i}[\Delta X_s(\eta,\ \zeta_j)-\Delta X_s(\eta,\ 0)]d\eta+F_{2ts}\int_0^{\zeta_j}[\Delta X_s(\eta_i,\ \zeta)-\Delta X_s(0,\ \zeta)]d\zeta\right.$$
$$\left.+F_{3ts}\int_0^{\eta_i}\int_0^{\zeta_j}\Delta X_s(\eta,\ \zeta)d\eta d\zeta\right\}+\delta_{1t}\int_0^{\eta_i}\int_0^{\zeta_j}\Delta\overline{q}(\eta,\ \zeta)d\eta d\zeta=0 \quad\cdots\cdots(3)$$

By applying the numerical integration to Eq. (3), a simultaneous equation of unknown quantities X_{sij} ($s=1\sim8$) which are the dimensionless shear forces, twisting moment, bending moments, rotations and deflection at the main point (i, j) of the area $[i, j]$ is obtained as follows:

$$\sum_{s=1}^{8}\left\{F_{1ts}\sum_{k=0}^{i}\beta_{ik}[\Delta X_{skj}-\Delta X_{sk0}]+F_{2ts}\sum_{l=0}^{j}\beta_{jl}[\Delta X_{sil}-\Delta X_{s0l}]+F_{3ts}\sum_{k=0}^{i}\sum_{l=0}^{j}\beta_{ik}\beta_{jl}\Delta X_{skl}\right\}$$
$$+\delta_{1t}\sum_{k=0}^{i}\sum_{l=0}^{j}\beta_{ik}\beta_{jl}\Delta\overline{q}_{kl}=0 \quad\cdots\cdots(4)$$

where $\overline{q}_{kl}$ is the value of function $\overline{q}(\eta, \zeta)$ at point (k, l).

The solution X_{pij} to the simultaneous Eq. (4) is expressed as follows:

$$\Delta X_{pij}=\sum_{t=1}^{8}\left\{\sum_{k=0}^{i}A_{pt}\beta_{ik}[\Delta X_{tkj}-\Delta X_{tk0}(1-\delta_{ki})]+\sum_{l=0}^{j}B_{pt}\beta_{jl}[\Delta X_{til}-\Delta X_{ti0}(1-\delta_{lj})]\right.$$
$$\left.+\sum_{k=0}^{i}\sum_{l=0}^{j}C_{ptkl}\beta_{ik}\beta_{jl}\Delta X_{tkl}(1-\delta_{ki}\delta_{lj})\right\}-A_{pt}\sum_{k=0}^{i}\sum_{l=0}^{j}\beta_{ik}\beta_{jl}\Delta\overline{q}_{kl} \quad\cdots\cdots(5)$$

where $p=1, 2, \cdots, 8$, $i=1, 2, \cdots, m$, $j=1, 2, \cdots, n$, $\beta_{ik}=\alpha_{ik}/m$, $\beta_{jl}=\alpha_{jl}/n$, A_{pt}, B_{pt}, C_{ptkl}: APPENDIX Ⅲ.

The coefficients β_{ik}, β_{jl} are the weight coefficients of numerical integration. The trapezoidal rule of approximate numerical integration are applied in this paper, therefore the values of α_{ik}, α_{jl} are given as follows:

$\alpha_{ik}=1-(\delta_{0k}+\delta_{ik})/2$, $\alpha_{jl}=1-(\delta_{0l}+\delta_{jl})/2$

In Eq. (5), the quantity X_{pij} at the main point (i, j) of the area $[i, j]$ is related to the quantities X_{ik0} and X_{t0l} at the boundary dependent points of the area $[i, j]$ and the quantities X_{tkj}, X_{til} and X_{tkl} at the inner dependent points of the area $[i, j]$. With the spreading of the area $[i, j]$ according to regular order as $[1, 1]$, $[1, 2]$, $\cdots$, $[1, n]$, $[2, 1]$, $[2, 2]$, $\cdots$, $[2, n]$, $\cdots$, $[m, 1]$, $[m, 2]$, $\cdots$, $[m, n]$, the main point of smaller area becomes one of the inner dependent points of the following larger areas. Whenever one obtains the quantity X_{pij} at the main point (i, j) of the area $[i, j]$ by using Eq. (5) in above mentioned order, one can eliminate the quantities X_{tkj}, X_{til} and X_{tkl} at the inner dependent points of the following larger areas by substituting the obtained results into the corresponding terms of the right hand side of Eq. (5). By repeating this process, the quantity X_{pij} at the main point is related to only the quantities X_{ik0} and X_{t0l} at the boundary dependent points. The results are as follows:

$$\Delta X_{pij}=\sum_{f=0}^{i}\{a_{pijf1}(\Delta Q_y)_{f0}+a_{pijf2}(\Delta M_{xy})_{f0}+a_{pijf3}(\Delta M_y)_{f0}+a_{pijf4}(\Delta\theta_y)_{f0}+a_{pijf5}(\Delta\theta_x)_{f0}+a_{pijf6}(\Delta w)_{f0}\}$$
$$+\sum_{g=0}^{j}\{b_{pijg1}(\Delta Q_x)_{0g}+b_{pijg2}(\Delta M_{xy})_{0g}+b_{pijg3}(\Delta M_x)_{0g}+b_{pijg4}(\Delta\theta_y)_{0g}+b_{pijg5}(\Delta\theta_x)_{0g}+b_{pijg6}(\Delta w)_{0g}\}$$
$$+\Delta q_{pij} \quad\cdots\cdots(6)$$

where integral constants: $(Q_y)=X_1$, $(Q_x)=X_2$, $(M_{xy})=X_3$, $(M_y)=X_4$, $(M_x)=X_5$, $(\theta_y)=X_6$, $(\theta_x)=X_7$, $(w)=X_8$, a_{pijfd}, b_{pijgd}, q_{pij}: APPENDIX Ⅳ.

Eq. (6) can be recognized as the discrete solutions of the fundamental partial differential Eq. (2).

4. INTEGRAL CONSTANTS AND BOUNDARY CONDITIONS

The integral constants mean the quantities at the discrete points along the edges $y=0$ ($\zeta=0$) and $x=0$ ($\eta=0$) of the rectangular plate. There are six integral constants at each discrete point, and three of them

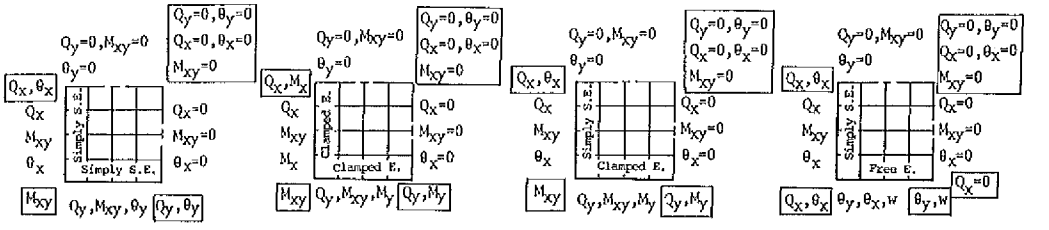

(1) SSSS (2) CCCC (3) SCSC (4) SFSF

Fig. 3 Integral Constants and Boundary Conditions.

are self-evident according to the boundary conditions along the edges $y=0$ and $x=0$. The remaining three integral constants can be determined by the boundary conditions along the edges $y=b$ and $x=a$.

The integral constants and the boundary conditions of rectangular plate with four simply supported edges (SSSS), four clamped edges (CCCC), two opposite edges simply supported and the other two edges clamped (SCSC), and two opposite edges simply supported and the other two edges free (SFSF) are shown in Fig. 3(1)~(4), respectively. These figures represent one quarter of the rectangular plate with two symmetrical axes. The integral constants and the boundary conditions at the corners of each plate are shown in the boxes. For the details of dealing with the integral constants and boundary conditions, see Ref. 12).

5. COMPUTATIONAL PROCEDURE

In this paper, the main assumptions are that : (a) displacement is small compared with the plate thickness ; (b) the stress normal to the midsurface of the plate is negligible ; (c) normals to the midsurface before deformation remain straight but not necessarily normal to the midsurface after deformation ; (d) Prandtl-Reuss's law obeying the von Mises yield criterion is assumed ; (e) the plate is made of non-hardening elasto-plastic material.

For the elasto-plastic analysis by the discrete method, an incremental variable elasticity procedure has been used. This procedure has many advantages in rapidity of convergence when materials with very flat stress-strain diagrams are used. Generally, it suffices to take the elasto-plastic stress-strain relations corresponding to the initial stress levels at the start of an increment (Ref. 13)). In order to consider the extension of the yielded portions in the directions of thickness of the element, it is divided into many layers (Fig. 4).

In the previous increment : $[n-1]$-st load incremental step

$$[\text{DATA}]\quad \frac{\sigma_x}{\sigma_0}=\sum^{n-1}\frac{\Delta\sigma_x}{\sigma_0},\ \frac{\sigma_y}{\sigma_0}=\sum^{n-1}\frac{\Delta\sigma_y}{\sigma_0},\ \frac{\tau_{xy}}{\sigma_0}=\sum^{n-1}\frac{\Delta\tau_{xy}}{\sigma_0} \qquad (7)$$

$\bar{\sigma}=(\sigma_x^2+\sigma_y^2-\sigma_x\sigma_y+3\tau_{xy}^2)^{\frac{1}{2}}$: σ_0, $\bar{\sigma}$: equivalent stress, σ_0 : yield stress

If in the previous increment the plastic range in the section has been created, an elasto-plastic stress-strain relation has to be used (loading), and if in the previous increment a decrease of strain occurred, then an elastic stress-strain relation is inserted for the present increment (unloading). The load is considered to be applied in incrementally, but the total strain occurring during the increment is treated, by the use of a suitably modified modulus, as if the material was elastic.

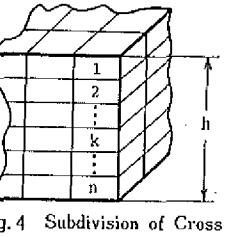

Fig. 4 Subdivision of Cross Section into Layers.

In the present increment : $[n]$-th load incremental step

(1) Nondimensional deviatoric stress

$$\bar{\sigma}'_x=\frac{1}{3}\left(2\frac{\sigma_x}{\sigma_0}-\frac{\sigma_y}{\sigma_0}\right),\ \bar{\sigma}'_y=\frac{1}{3}\left(2\frac{\sigma_y}{\sigma_0}-\frac{\sigma_x}{\sigma_0}\right),\ \bar{\tau}'_{xy}=\frac{\tau_{xy}}{\sigma_0} \qquad (8)$$

$\bar{\sigma}'_x=\sigma'_x/\sigma_0$, $\bar{\sigma}'_y=\sigma'_y/\sigma_0$, $\bar{\tau}'_{xy}=\tau'_{xy}/\sigma_0$

(2) $a=\overline{\sigma}'_x+\nu\overline{\sigma}'_y,\ b=\nu\overline{\sigma}'_x+\overline{\sigma}'_y,\ c=(1-\nu)\overline{\tau}'_{xy},\ d=a\overline{\sigma}'_x+b\overline{\sigma}'_y+2c\overline{\tau}'_{xy}$ ..... (9)

(3) $$\begin{bmatrix} \alpha_{11} & \alpha_{12} & \alpha_{13} \\ \alpha_{21} & \alpha_{22} & \alpha_{23} \\ \alpha_{31} & \alpha_{32} & \alpha_{33} \end{bmatrix} = \begin{bmatrix} 1 & \nu & 0 \\ \nu & 1 & 0 \\ 0 & 0 & (1-\nu)/2 \end{bmatrix} - \frac{1}{d}\begin{bmatrix} a^2 & ab & ac \\ ab & b^2 & bc \\ ac & bc & c^2 \end{bmatrix}$$ ..... (10)

(4) $a_{ij}=12h^3\int_{-\frac{1}{2}}^{\frac{1}{2}}\alpha_{ij}\xi^2 d\xi$ ..... (11)

(5) $[b_{ij}]=[a_{ij}]^{-1}$ ..... (12)

(6) The incremental moments $\Delta M_x,\ \Delta M_y,\ \Delta M_{xy}$ are calculated by the discrete solutions.

(7) $$\begin{bmatrix} \Delta\beta_x \\ \Delta\beta_y \\ \Delta\beta_{xy} \end{bmatrix} = \frac{1}{D}\begin{bmatrix} \alpha_{11} & \alpha_{12} & \alpha_{13} \\ \alpha_{21} & \alpha_{22} & \alpha_{23} \\ \alpha_{31} & \alpha_{32} & \alpha_{33} \end{bmatrix}^{-1}\begin{bmatrix} \Delta M_x \\ \Delta M_y \\ \Delta M_{xy} \end{bmatrix}$$ ..... (13)

$$\begin{bmatrix} \Delta\sigma_x/\sigma_0 \\ \Delta\sigma_y/\sigma_0 \\ \Delta\tau_{xy}/\sigma_0 \end{bmatrix} = \frac{E\cdot z}{(1-\nu^2)\sigma_0}\begin{bmatrix} \alpha_{11} & \alpha_{12} & \alpha_{13} \\ \alpha_{21} & \alpha_{22} & \alpha_{23} \\ \alpha_{31} & \alpha_{32} & \alpha_{33} \end{bmatrix}\begin{bmatrix} \Delta\beta_x \\ \Delta\beta_y \\ \Delta\beta_{xy} \end{bmatrix}$$ ..... (14)

(8) $\frac{\sigma_x}{\sigma_0}=\sum^{n}\frac{\Delta\sigma_x}{\sigma_0},\ \frac{\sigma_y}{\sigma_0}=\sum^{n}\frac{\Delta\sigma_y}{\sigma_0},\ \frac{\tau_{xy}}{\sigma_0}=\sum^{n}\frac{\Delta\tau_{xy}}{\sigma_0}$ ..... (15)

6. NUMERICAL RESULTS

Numerical solutions for four specific problems are presented. All four problems involve square plates subjected to lateral loads that are uniformly distributed throughout the plate. From the results of the elastic bending analysis of variable thickness plates (Ref. 14)) and the elasto-plastic analysis of the four edges simply supported plates which is divided into $m=n=4$, 6, 8, 10, the elasto-plastic numerical solutions converged with the divisional meshes $m=n=8$. And the number of layers in the direction of the cross section was $nz=20$, from the results of the elasto-plastic analysis of the plate which is divided into $nz=10$, 20, 30, 40 (Ref. 14)). Moreover, the number of layers is hardly affected by computer storage and time.

(1) Simply supported plate (SSSS)

First, in order to confirm the convergency and accuracy of the numerical solutions obtained by the discrete method, let it be applied to the elasto-plastic analysis of the square plate with four simple supported edges under uniform load. The results are summarized in Figs. 5 through 7. Fig. 5 shows the load-deflection curves with respect to the maximum deflection when nondimensional incremental load intensity is $\Delta qa^2/M_p=2.0$, 1.0, 0.4, 0.2 ($M_p=\sigma_0 h^2/4$: fully plastic moment). This figure also shows a comparison among the discrete solution and the finite difference solutions obtained by Bhaumik and Hanley[9] and the finite element solution by Owen and Hinton[8]. It is found from this figure that the numerical

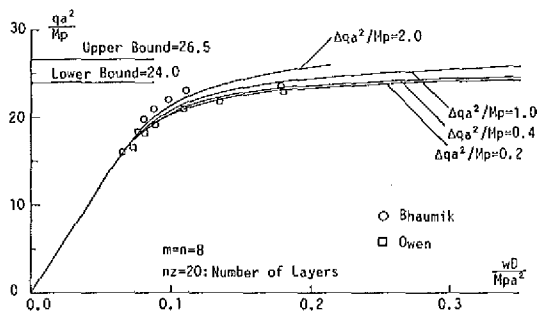

Fig. 5 Load-Deflection Curves for Simply Supported Square Plate.

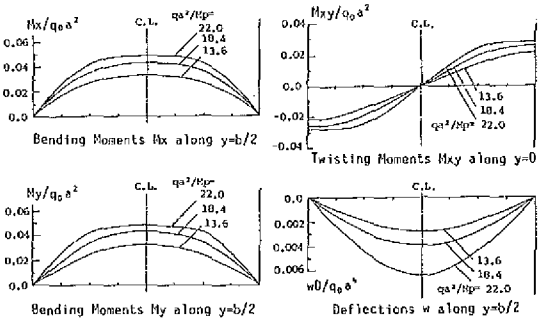

Fig. 6 Typical Moment and Deflection Diagrams for Simply Supported Square Plate.

solutions obtained by the discrete method (when $\Delta q a^2/M_p=0.2$) agree with those obtained by the finite element and the finite difference method. Spatial redistributions of moments and deflection are illustrated in Fig. 6 for three levels of loading. It is found from this figure that spatial redistribution of moments is smooth according to the extent of the plastic region. Fig. 7 shows the progression of the plastic regions at different levels of loading. From this figure, first yielding is observed at the four corners of the plate and then at the center, and the plastic regions extend along the diagonals. In this paper, h/h_0 represents the elastic portions in the directions of thickness of the element. ($h/h_0=1.0$: fully elastic portion, $h/h_0=0.0$: fully plastic portion)

(2) Plate supported with clamps (CCCC)

In Figs. 8 through 10 are presented the corresponding results for a square plate with all edges clamped. Fig. 8 shows the load-deflection curve with respect to maximum deflection. In Fig. 8, the numerical solutions obtained from the discrete method are compared with those of the finite difference method[3], a good agreement exists between these sets of results. Fig. 9 illustrates the redistribution of moments and deflection for three levels of loading. The progressions of the yield regions at different levels of loading is summarized in Fig. 10. In this case, the first yielding of the plate occurs at the middle of the four edges, and the plastic regions extend along these edges until the center of the plate yields.

(3) Plate with two edges clamped (SCSC)

Results similar to those described above for a square plate with two opposite edges simply supported and the other two edges clamped are described in Figs. 11 through 13. Fig. 11 shows the load-deflection curve with respect to maximum deflection. The redistribution of moments and deflection are illustrated in Fig. 12, and the progression of the yield regions is summarized in Fig. 13.

(4) Plate with two edges free (SFSF)

In Figs. 14 through 16 are presented the corresponding results for a square plate with two opposite edges simply supported and the other two edges free. Fig. 14 shows the load-deflection curve with respect to

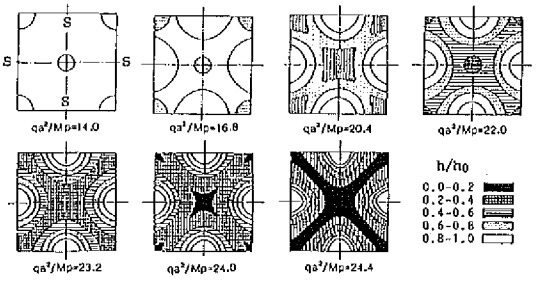

Fig. 7 Progression of Yield Regions (SSSS).

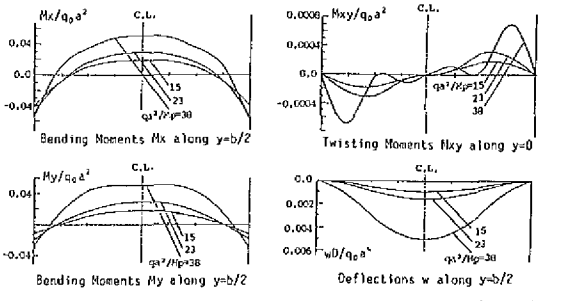

Fig. 9 Typical Moment and Deflection Diagrams for Clamped Square Plate.

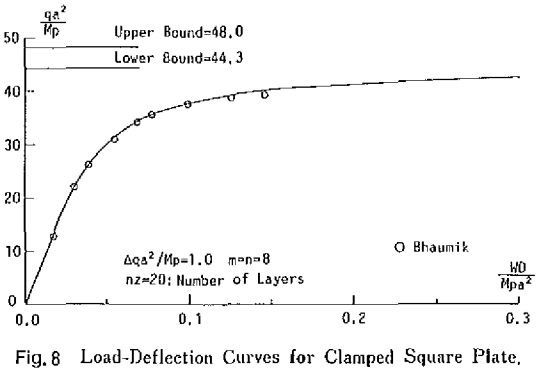

Fig. 8 Load-Deflection Curves for Clamped Square Plate.

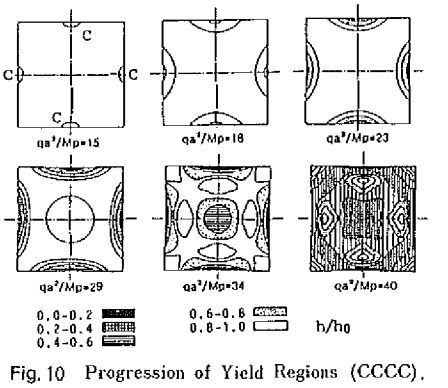

Fig. 10 Progression of Yield Regions (CCCC).

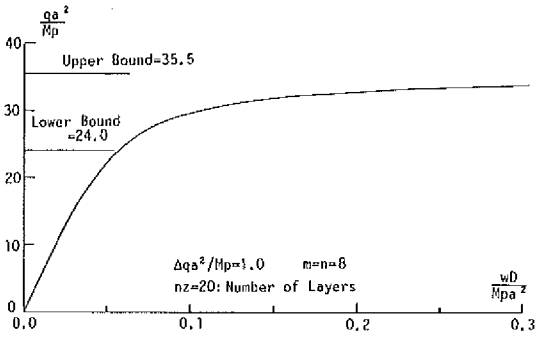

Fig. 11 Load-Deflection Curves for Square Plate with Two Opposite Edges Simply Supported and the Other Two Edges Clamped.

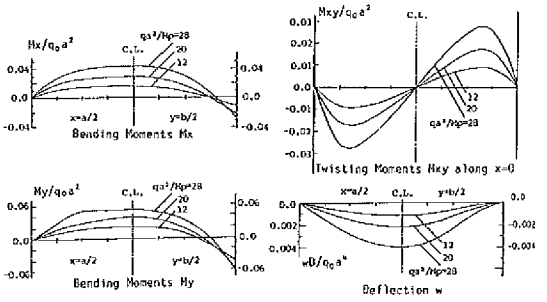

Fig. 12 Moment and Deflection Diagrams for Square Plate with Two Opposite Edges Simply Supported and the Other Two Edges Clamped.

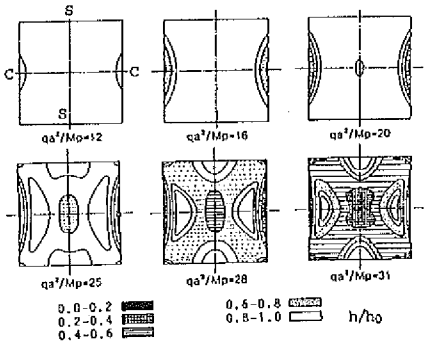

Fig. 13 Progression of Yield Regions (SCSC).

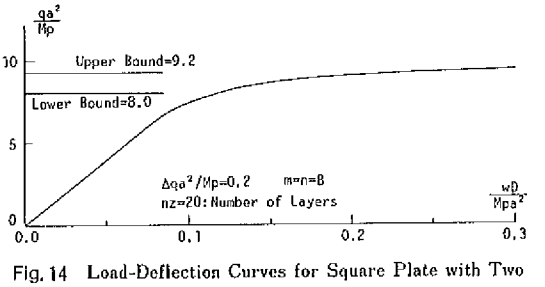

Fig. 14 Load-Deflection Curves for Square Plate with Two Opposite Edges Simply Supported and the Other Two Edges Free.

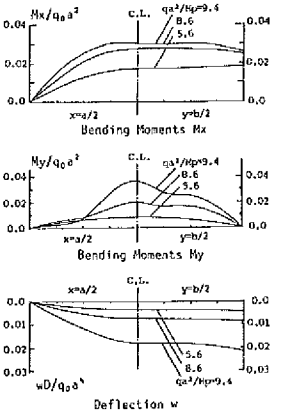

Fig. 15 Moment and Deflection Diagrams (SFSF).

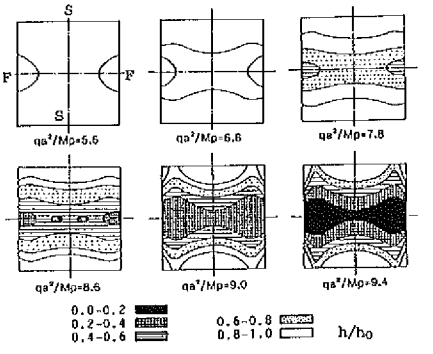

Fig. 16 Progression of Yield Regions (SFSF).

maximum deflection. The redistribution of moments and deflection are illustrated in Fig. 15, and the progression of the yield regions is summarized in Fig. 16.

7. CONCLUSIONS

The main conclusions of the work described in this paper are summarized as follows.

(1) A general numerical method for the elasto-plastic bending of rectangular plate has been proposed, and the proposed method has been applied to the square plates with four types of boundary conditions.

(2) The discrete solutions are obtained by transforming the differential equations into integral equations and applying numerical integrations, and they give the transverse shear forces, twisting moments, bending moments, rotations and deflections at all the discrete points which are the intersection

of the vertical and horizontal equally dividing lines on the plate. Thus, the proposed method does not require prior assumption of the shape of the deflection of the plate.

(3) By utilizing the present method, the elasto-plastic problems for the rectangular plates having various boundary conditions can be treated with acceptable accuracy.

APPENDIX I

$$[b_{ij}]=[a_{ij}]^{-1},\quad [a_{ij}]=12\int_{-\frac{1}{2}}^{\frac{1}{2}}[\alpha_{ij}]\xi^2 d\xi,\quad \begin{bmatrix}\alpha_{11}&\alpha_{12}&\alpha_{13}\\ \alpha_{21}&\alpha_{22}&\alpha_{23}\\ \alpha_{31}&\alpha_{32}&\alpha_{33}\end{bmatrix}=\begin{bmatrix}1&\nu&0\\ \nu&1&0\\ 0&0&(1-\nu)/2\end{bmatrix}^{-\frac{1}{a}}\begin{bmatrix}a^2&ba&ca\\ ab&b^2&cb\\ ac&bc&c^2\end{bmatrix}$$

a, b, c, d : refer to Eqs. (8) and (9)

APPENDIX II

$F_{111}=F_{123}=F_{134}=F_{156}=F_{167}=F_{188}=F_{278}=F_{377}=1.0$,
$F_{212}=F_{225}=F_{233}=F_{247}=F_{266}=F_{386}=-F_{322}=-F_{331}=\mu$, $F_{345}=-b_{11}I$, $F_{344}=-b_{12}I$, $F_{343}=-b_{13}I$,
$F_{355}=-b_{21}I$, $F_{354}=-b_{22}I$, $F_{353}=-b_{23}I$, $F_{365}=-b_{31}I$, $F_{364}=-b_{32}I$, $F_{363}=-b_{33}I$,
$F_{372}=-K$, $F_{381}=-\mu K$, other $F_{ijk}=0$, $I=\mu(1-\nu^2)(h_0/h)^3$, $K=(h_0/a)^2\cdot(h_0/h)E/(12\,xG)$

APPENDIX III

$\rho_{11}=\beta_{ii}$, $\rho_{12}=\mu\beta_{jj}$, $\rho_{22}=-\mu\beta_{ij}$, $\rho_{23}=\beta_{ii}$, $\rho_{25}=\mu\beta_{jj}$, $\rho_{31}=-\mu\beta_{ij}$, $\rho_{33}=\mu\beta_{jj}$, $\rho_{34}=\beta_{ii}$,
$\rho_{43}=-I_{ij}\beta_{ij}b_{13ij}$, $\rho_{44}=-I_{ij}\beta_{ij}b_{12ij}$, $\rho_{45}=-I_{ij}\beta_{ij}b_{11ij}$, $\rho_{47}=\mu\beta_{jj}$, $\rho_{53}=-I_{ij}\beta_{ij}b_{23ij}$, $\rho_{54}=-I_{ij}\beta_{ij}b_{22ij}$,
$\rho_{55}=-I_{ij}\beta_{ij}b_{21ij}$, $\rho_{56}=\beta_{ii}$, $\rho_{63}=-I_{ij}\beta_{ij}b_{33ij}$, $\rho_{64}=-I_{ij}\beta_{ij}b_{32ij}$, $\rho_{65}=-I_{ij}\beta_{ij}b_{31ij}$, $\rho_{66}=\mu\beta_{jj}$, $\rho_{67}=\beta_{ii}$,
$\rho_{72}=-\beta_{ij}K_{ij}$, $\rho_{77}=\beta_{ij}$, $\rho_{78}=\beta_{jj}$, $\rho_{81}=-\mu\beta_{ij}K_{ij}$, $\rho_{86}=\mu\beta_{ij}$, $\rho_{88}=\beta_{ii}$, $\beta_{ij}=\beta_{ii}\cdot\beta_{jj}$
$[\gamma_{pt}]=[\rho_{tp}]^{-1}$

$A_{p1}=\gamma_{p1}$ $B_{p1}=0$ $C_{p1kl}=\mu\gamma_{p3}+\gamma_{p8}\mu K_{kl}$
$A_{p2}=0$ $B_{p2}=\mu\gamma_{p1}$ $C_{p2kl}=\mu\gamma_{p2}+\gamma_{p7}K_{kl}$
$A_{p3}=\gamma_{p2}$ $B_{p3}=\mu\gamma_{p3}$ $C_{p3kl}=I_{kl}(\gamma_{p4}b_{13kl}+\gamma_{p5}b_{23kl}+\gamma_{p6}b_{33kl})$
$A_{p4}=\gamma_{p3}$ $B_{p4}=0$ $C_{p4kl}=I_{kl}(\gamma_{p4}b_{12kl}+\gamma_{p5}b_{22kl}+\gamma_{p6}b_{32kl})$
$A_{p5}=0$ $B_{p5}=\mu\gamma_{p2}$ $C_{p5kl}=I_{kl}(\gamma_{p4}b_{11kl}+\gamma_{p5}b_{21kl}+\gamma_{p6}b_{31kl})$
$A_{p6}=\gamma_{p5}$ $B_{p6}=\mu\gamma_{p6}$ $C_{p6kl}=-\mu\gamma_{p8}$
$A_{p7}=\gamma_{p6}$ $B_{p7}=\mu\gamma_{p4}$ $C_{p7kl}=-\gamma_{p7}$
$A_{p8}=\gamma_{p8}$ $B_{p8}=\gamma_{p7}$ $C_{p8kl}=0$

APPENDIX IV

$$a_{pijfd}=\sum_{t=1}^{8}\Big\{A_{pt}\sum_{k=0}^{i}\beta_{ik}[a_{tk0fd}-a_{tkjfd}(1-\delta_{ki})]+B_{pt}\sum_{l=0}^{j}\beta_{jl}[a_{ti0lfd}-a_{tilfd}(1-\delta_{lj})]$$
$$+\sum_{k=0}^{i}\sum_{l=0}^{j}C_{ptkl}\beta_{ik}\beta_{jl}a_{tiklfd}(1-\delta_{ki}\delta_{lj})\Big\}$$

$$b_{pijgd}=\sum_{t=1}^{8}\Big\{A_{pt}\sum_{k=0}^{i}\beta_{ik}[b_{tk0gd}-b_{tkjgd}(1-\delta_{ki})]+B_{pt}\sum_{l=0}^{j}\beta_{jl}[b_{ti0gd}-b_{tilgd}(1-\delta_{lj})]$$
$$+\sum_{k=0}^{i}\sum_{l=0}^{j}C_{ptkl}\beta_{ik}\beta_{jl}b_{tiklgd}(1-\delta_{ki}\delta_{lj})\Big\}$$

$$q_{pij}=\sum_{t=1}^{8}\Big\{A_{pt}\sum_{k=0}^{i}\beta_{ik}[q_{tk0}-q_{tkj}(1-\delta_{ki})]+B_{pt}\sum_{l=0}^{j}\beta_{jl}[q_{ti0}-q_{til}(1-\delta_{lj})]$$
$$+\sum_{k=0}^{i}\sum_{l=0}^{j}C_{ptkl}\beta_{ik}\beta_{jl}q_{tkl}(1-\delta_{ki}\delta_{lj})\Big\}-A_{p1}\sum_{k=0}^{i}\sum_{l=0}^{j}\beta_{ik}\beta_{jl}\bar{q}_{kl}$$

$$b_{5i003}=\frac{1}{t_{11}(i,0)}\frac{\bar{D}_{00}}{\bar{D}_{i0}}\bar{\alpha}_i,\quad a_{40j03}=\frac{1}{t_{22}(0,j)}\frac{\bar{D}_{00}}{\bar{D}_{0j}}\bar{\alpha}_j,\quad a_{5i0k3}=-\frac{t_{12}(k,0)}{t_{11}(i,0)}\frac{\bar{D}_{k0}}{\bar{D}_{i0}}\bar{\beta}_{ik}$$

$$b_{40Jl3}=-\frac{t_{21}(0,\,l)}{t_{22}(0,\,j)}\frac{\overline{D}_{0l}}{\overline{D}_{0j}}\bar{\beta}_{jl},\quad a_{5i0k2}=-\frac{t_{13}(k,\,0)}{t_{11}(i,\,0)}\frac{\overline{D}_{k0}}{\overline{D}_{i0}}\bar{\beta}_{ik},\quad b_{40Jl2}=-\frac{t_{23}(0,\,l)}{t_{22}(0,\,j)}\frac{\overline{D}_{0l}}{\overline{D}_{0j}}\bar{\beta}_{jl}$$

$$a_{5i0k5}=\frac{1}{(1-\nu^2)\overline{D}_{i1}\,t_{11}(i,\,0)}\bar{\gamma}_{ik},\quad b_{40Jl4}=\frac{1}{\mu(1-\nu^2)\overline{D}_{1j}\,t_{22}(0,\,j)}\bar{\gamma}_{jl}$$

$$a_{10Jl1}=\frac{K_{00}}{K_{0j}}\bar{\alpha}_j,\quad b_{10Jl4}=\frac{1}{K_{0j}}\bar{\beta}_{jl},\quad b_{10Jl6}=\frac{1}{\mu K_{0j}}\bar{\gamma}_{jl},\quad b_{2i001}=\frac{K_{00}}{K_{i0}}\bar{\alpha}_i,\quad a_{2i0k5}=\frac{1}{K_{i0}}\bar{\beta}_{ik},\quad a_{2i0k6}=\frac{1}{K_{i0}}\bar{\gamma}_{ik}$$

$$[t_{ij}]=[a_{ij}]^{-1}$$

$$\bar{\alpha}_i=(-1)^i,\quad \bar{\alpha}_j=(-1)^j,\quad \overline{D}_{i0}=D_0/D_{i0},\quad \bar{\beta}_{ik}=\delta_{ik}+(-1)^{i+1}\cdot\delta_{0k},\quad \bar{\beta}_{jl}=\delta_{jl}+(-1)^{j+1}\cdot\delta_{0l}$$

$$\bar{\gamma}_{ik}=\frac{4\,m(-1)^{i+k}}{1+\delta_{ik}+\delta_{0k}},\quad \bar{\gamma}_{jl}=\frac{4\,n(-1)^{j+l}}{1+\delta_{jl}+\delta_{0l}},\quad \bar{\gamma}_{ik}=\begin{cases}0 & (i<k)\\ \bar{\gamma}_{ik} & (i\geqq k)\end{cases},\quad \bar{\gamma}_{jl}=\begin{cases}0 & (j<l)\\ \bar{\gamma}_{jl} & (j\geqq l)\end{cases}$$

REFERENCES

1) Hodge, P. G. : Plastic Analysis of Structures, Corona Publishing Co., Ltd., 1961 (in Japanese).
2) Kusuda, T. : Plastic analysis of plate structures subjected to transverse load, Journal of the Society of Naval Architects of Japan, No. 107, pp. 195~202, 1960 (in Japanese).
3) Bhaumick, A. K. and Hanlay, J. T. : Elasto-plastic plate analysis by finite differences, Journal of Structural Division, Proc. of ASCE, Vol. 93, No. ST 5, pp. 279~294, 1967.
4) Yokoo, Y., Nakamura, T. and Mori, T. : Numerical analysis of elastic-plastic deformation of simply supported rectangular plates, Trans. of A. I. J. No. 152, pp. 27~36, 1968.
5) May, G. W. and Gerstle, K. H. : Elastic-plastic bending of rectangular plate, Journal of Engineering Mechanics Division, Proc. ASCE, Vol. 94, No. EM1, pp. 199~210, 1968.
6) Ang, A. H. S. and Lopez, L. A. : Discrete model analysis of elastic-plastic plates, Journal of Structural Division, Proc. of ASCE, Vol. 97, No. ST7, pp. 1863~1878, 1968.
7) Komatsu, S., Kitada, T. and Miyazaki, S. : Elasto-plastic analysis of compressed plate with residual stress and initial deflection, Proc. of the Japan Society of Civil Engineers, No. 244, pp. 1~14, 1975 (in Japanese).
8) Owen, D. R. J. and Hinton, E. : Finite Elements in Plasticity, Pineridge Press Limited, Swansea, U. K., pp. 319~373, 1980.
9) Oblak, M. : Elasto-plastic bending analysis of a thick plate, ZAMM, Vol. 66, pp. 320~322, 1986.
10) Ohga, M., Shigematsu, T. and Hara, T. : Combined finite element-transfer matrix method, Journal of Engineering Mechanics Division, Proc. ASCE, Vol. 110, No. EM9, pp. 1335~1349, 1984.
11) Lin, T. H. and Ho, E. Y. : Elasto-plastic bending of rectangular plate, Journal of Engineering Mechanics Division, Proc. ASCE, Vol. 94, No. EM1, pp. 199~210, 1968.
12) Sakiyama, T. and Matsuda, H. : Bending analysis of rectangular plate with variable thickness, Proc. of the Japan Society of Civil Engineers, No. 338, pp. 21~28, 1983 (in Japanese).
13) Zienkiewicz, O. C. and Cheung, Y. K. : The Finite Element Method in Structural and Continuum Mechanics, McGraw-Hill Publishing Company Limited, pp. 198~201, 1967.
14) Matsuda, H. and Sakiyama, T. : Numerical Analysis of Inelastic Behaviour of Rectangular Plate, Journal of Structural Engineering, Vol. 33 A, pp. 257~264, 1987 (in Japanese).

(Received June 25 1987)